Dalton Transactions

Reversible Hydrogen Adsorption at Room Temperature using Molybdenum-Dihydrogen Complex in Solid State

Journal:	*Dalton Transactions*
Manuscript ID	DT-ART-04-2021-001404.R2
Article Type:	Paper
Date Submitted by the Author:	31-Jul-2021
Complete List of Authors:	Uchida, Kaiji; Tohoku University, Chemistry Kishimoto, Naoki; Tohoku University, Chemistry Noro, Shin-ichiro; Hokkaido University, Faculty of Environmental Earth Science Iguchi, Hiroaki; Tohoku University, Department of Chemistry, Graduate School of Science Takaishi, Shinya; Tohoku University, Chemistry

ARTICLE

Reversible Hydrogen Adsorption at Room Temperature using Molybdenum-Dihydrogen Complex in Solid State

Received 00th January 20xx,
Accepted 00th January 20xx

DOI: 10.1039/x0xx00000x

Kaiji Uchida,[a] Naoki Kishimoto,[a] Shin-ichiro Noro,[b] Hiroaki Iguchi,[a] and Shinya Takaishi*[a]

Reversible H_2 storage under a mild condition is one of the most important targets in the field of materials chemistry. Dihydrogen complexes are the attractive materials for this target because they possess moderate adsorption enthalpy as well as adsorption without cleavage of H-H bond. In spite of these advantages, H_2 adsorption studies of the dihydrogen complexes in the solid state are scarce. We herein present H_2 adsorption properties of the 16-electron precursor complex ($[Mo(PCy_3)_2(CO)_3]$) in the solid state synthesized by the two procedures. One is direct synthesis under Ar atmosphere (**1**), the other is removal of the N_2-adduct under vacuum (**2**). **2** showed ideal Langmuir type reversible ad/desorption of H_2 above room temperature, whereas **1** showed irreversible adsorption. The adsorption enthalpy of **2** was larger than that in the THF solution. Using DFT calculation, this difference was explained by the absence of the agostic interaction in the solid state.

Introduction

Due to the growing interest toward energy and environmental problems, pursuit of clean energy source for sustainable society is intense around the world. Dihydrogen H_2 has extremely large energy density (120 MJ/kg vs 44.5 MJ/kg for gasoline) and environment-friendly (CO_2-free) power production is possible by using fuel cell. Because of these characteristics, H_2 is one of the best candidates as a future energy source. On the other hand, it is quite difficult to store H_2 under a mild condition due to extremely small density, small intermolecular interactions, and resultant low boiling point.

To solve this problem, many kinds of materials including metal-organic frameworks (MOFs),[1-11] covalent organic frameworks (COFs),[12] chemical hydrides[13-15] and hydrogen-absorbing alloys[16] have been studied intensely for H_2 storage. These solid-state H_2 storage materials are roughly divided into physisorptive and chemisorptive mechanisms, and each has pros and cons. Physisorptive materials have extremely low H_2 uptake under ambient conditions due to low adsorption enthalpy ($|\Delta H°| < 10$ kJ/mol), while the interaction with hydrogen is reversible and kinetics is fast. On the other hand, chemisorptive materials can adsorb H_2 under ambient conditions by forming a strong chemical bond with hydrogen, but at the same time, this process is accompanied by the cleavage of H-H bond, which leads to irreversible adsorption and extremely slow kinetics at room temperature. So the exploration of intermediate of these two mechanisms is necessary for developing reversible H_2 ad/desorption materials under a mild condition.

Metal-dihydrogen complexes are the appealing candidates because of their moderate adsorption enthalpy which ranges from –25 to –50 kJ/mol. First metal-dihydrogen complex was reported by Kubas and coworkers in 1984,[17] and hundreds of compounds were reported so far.[18-27] Orbital interaction of metal-dihydrogen complex is described in the same manner as Dewar-Chatt-Duncanson model, namely, η^2 type M-H_2 bond is formed by σ-donation from H_2 to metal and π-back-donation from metal to H_2. In the metal-dihydrogen complex, chemical bond is formed between metal and dihydrogen molecule, whereas H-H bond is kept albeit it is elongated and weakened. This can be regarded as an intermediate of physisorption and chemisorption, and therefore, large adsorption enthalpy and fast ad/desorption kinetics could be achieved. Actually, solution calorimetry study of $[W(PCy_3)_2(CO)_3]$ (PCy_3 = tricyclohexylphosphine) revealed that this complex has moderate enthalpy (≈ –40 kJ/mol) of H_2 binding in THF or toluene solution.[28] Also about the other metals, variable-temperature spectroscopic studies were also performed and their thermodynamic properties were thoroughly investigated in solution state.[29-32]

Recently, the η^2 coordination motif has been widely utilized for solid-state hydrogen storage materials.[5,9,33-41] As for the conventional dihydrogen complexes, on the other hand, there is only one example of the H_2 adsorption study on $[Mn(CO)(dppe)_2][BAr^F{}_4]$ (Ar^F = 3,5-$(CF_3)_2C_6H_3$)[42] in the solid state though several papers reported the dihydrogen complex formation,[43-45] to the best of our knowledge.

In this study, we studied the H_2 adorption of $[Mo(PCy_3)_2(CO)_3]$, a 16-electron precusor of one of the conventional dihydrogen complexes, in the solid state. We synthesized $[Mo(PCy_3)_2(CO)_3]$ in two different methods, namely a direct synthesis under Ar atmosphere (**1**) and removal of N_2-adduct under vacuum (**2**).

[a] *Department of Chemistry, Graduate School of Science, Tohoku University, Sendai 980-8578 (Japan).*
[b] *Faculty of Environmental Earth Science, Hokkaido University, Sapporo 060-0810 (Japan)*

Electronic Supplementary Information (ESI) available: [Experimental details, adsorption measurements, kinetic analyses and DFT calculations]. See DOI: 10.1039/x0xx00000x

Details are written in ESI. H_2 adsorption isotherms of each sample were measured at various temperature. Isotherms changed dramatically depending on the synthetic procedures, and large difference of adsorption enthalpy was found between in the solid state (this work) and in the THF or toluene solution (ref. 28). According to the density functional theory (DFT) calculation of $[Mo(PR_3)_2(CO)_3]$ (R = methyl, isopropyl and cyclohexyl), the enthalpy difference between them was reasonably explained by the absence of the agostic interaction in the solid state. In this paper, we report the synthesis, H_2 adsorption measurements and DFT calculation of $[Mo(PCy_3)_2(CO)_3]$.

Results and Discussion

H_2 ad/desorption isotherm at 333 K of **1** and **2** are shown in Fig. 1. Adsorption behaviours of **1** and **2** are quite different. **2** showed a type-I adsorption isotherm with a good linearity in a Langmuir plot (Fig. S2), indicating the existence of site-specific interaction between coordinatively-unsaturated Mo atom and dihydrogen molecule. Ad/desorption isotherms were fully reversible in measured pressure range. These data shows that the H_2 adsorption of **2** occurred by site-specific metal-dihydrogen complex formation in the solid state.

On the other hand, **1** showed an irreversible isotherm. This irreversible isotherm and increase of adsorbed amount in the pressure-reducing process indicates that the ad/desorption was quite slow so that equilibrium was not reached. The isotherms at other temperature also showed irreversible adsorption behaviour (Fig. S4). Due to the non-equilibrium adsorption behaviour, it was impossible to analyse the thermodynamic properties of **1**.

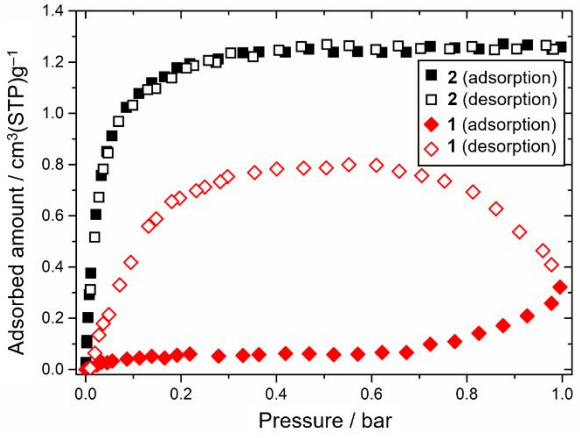

Fig. 1 H_2 adsorption isotherms of **1** and **2** at 333 K. Red diamond represents the data of **1** and black square represents the data of **2**. Filled and hollow symbols represent adsorption and desorption, respectively.

In order to clarify the origin of this difference, we measured N_2 adsorption of **1** and **2** at 77 K (Fig. S6 and S7). The BET surface area of **2** (3.6 m^2g^{-1}) was three times larger than that of **1** (1.2 m^2g^{-1}). In addition, the adsorption amount of **2** largely increased at $P/P_0 > 0.95$, suggesting that **2** was highly pulverized probably during the N_2 removal process, and it enabled H_2 molecule to approach the Mo centre at the polycrystalline surface.

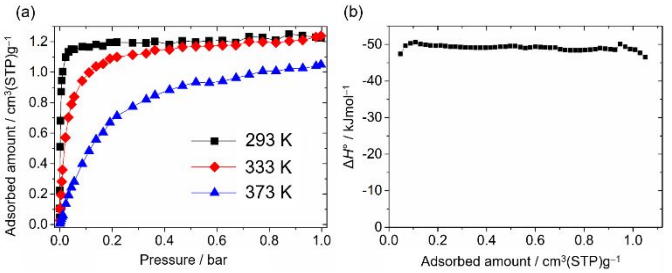

Fig. 2 (a) H_2 adsorption isotherms of **2** at 293, 333 and 373 K. (b) Adsorption enthalpy (ΔH) of **2** estimated using data at 293, 333, 373 K.

To investigate the thermodynamic properties of **2**, variable-temperature H_2 adsorption isotherms were measured. The data between 313 and 373 K are shown in Fig. 3 (see Fig. S1 for all the data). Saturation values of the adsorbed amount are in the range of 1.14–1.24 $cm^3(STP)g^{-1}$ at all temperature, corresponding to ~0.04 H_2 per Mo centre. This small value is attributed to the nonporous nature of $[Mo(PCy_3)_2(CO)_3]$, which was confirmed by N_2 adsorption isotherm at 77 K (Fig. S6). Ad/desorption cycle was repeated 4 times and no significant decrease of adsorbed amount was observed (Fig. S3), which indicates that $[Mo(PCy_3)_2(CO)_3]$ is stable up to 373 K in solid state.

Thermodynamic properties of H_2 adsorption were studied by analysing the adsorption isotherms. First, the adsorption enthalpy ($\Delta H°$) evaluated from isosteric differential heat of adsorption was calculated from the adsorption isotherms, and it was almost constant around –49 kJ/mol regardless of the surface coverage (Fig. 2). It indicates that H_2 adsorption in **2** is a single site adsorption and each site is independent of each other, which well obeys the Langmuir model. All isotherms were accurately fitted ($R^2 > 0.998$) by Langmuir adsorption isotherm,

$$\theta = \frac{V_a}{V_m} = \frac{KP}{1+KP} \quad (1)$$

where ϑ is the adsorbed fraction of the adsorbent, V_m is the mono-layer adsorption capacity and K is the Langmuir equilibrium constant. Obtained fitting parameters are listed in Table S1.

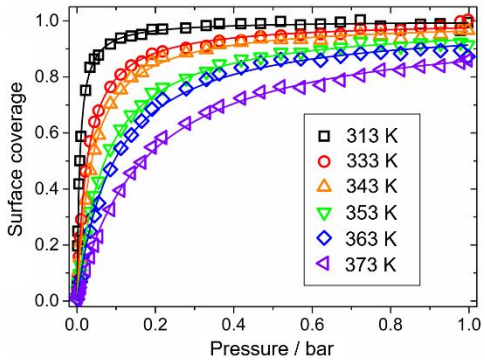

Fig. 3 Variable-temperature H_2 adsorption isotherms of **2**. Symbols represent the measured data and lines represent the fitting curves by Langmuir adsorption isotherm. Vertical axis is normalized to a surface coverage of the adsorbent.

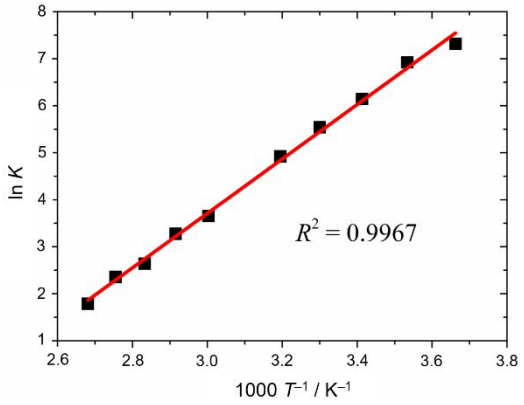

Fig. 4 van't Hoff plot of **2**. Black square represents the Langmuir equilibrium constant obtained from fitting and red line represents the fitted line by equation 2.

van't Hoff plot was made by using these values and fitted by following equation,

$$\ln K = -\frac{\Delta H^{\circ} 1}{R\ T} + \frac{\Delta S^{\circ}}{R} \quad (2)$$

where $\Delta H°$ is the standard molar enthalpy change of adsorption, $\Delta S°$ is the standard molar entropy change of adsorption and R is the ideal gas constant. Fitting of the van't Hoff plot gave following parameters; $\Delta H°$= − 48.1 kJ/mol and $\Delta S°$ = − 113.5 J · K/mol.

Absolute value of $\Delta S°$ is slightly smaller than standard molar entropy of free dihydrogen molecule (130.7 J · K/mol), which indicates that most of the entropic term derives from the suppression of translational and rotational motion of hydrogen, and small deviation is due to the newly appeared 6 vibrational mode by addition of the two hydrogen atoms to form [Mo(η^2-H_2)(PCy_3)$_2$(CO)$_3$], as well as the relatively free rotational motion of η^2-H_2 ligand. It is noteworthy that absolute value of $\Delta H°$ is significantly larger than reported value of $\Delta H°$ = –27.2 kJ/mol in variable-temperature spectroscopic study in THF solution. [28] To clarify the origin of the energy difference between solid state and solution state, DFT calculation was performed.

DFT calculation was performed to evaluate the energy difference between [Mo(PR_3)$_2$(CO)$_3$] (R = alkyl group) with and without agostic interaction. It has been reported that [Mo(PCy_3)$_2$(CO)$_3$] shows Mo-P-C-C-H···Mo type agostic interaction, in which β-hydrogen interact with Mo centre (β-agostic interaction).[46] We selected R = Cy and isopropyl (iPr) as a molecule with the agostic interaction, while R = methyl (Me) as a model without agostic interaction because PMe_3 has no β-hydrogen. The detail of calculation method is shown in experimental section (See ESI). Optimized structures of [Mo(PCy_3)$_2$(CO)$_3$] (Mo-PCy_3), [Mo($PiPr_3$)$_2$(CO)$_3$] (Mo-$PiPr_3$) and [Mo(PMe_3)$_2$(CO)$_3$] (Mo-PMe_3) are shown in Fig. S13-15. As can be seen from the figure, Mo-PCy_3 (and Mo-$PiPr_3$) have highly distorted structure with P-Mo-P angle of 166.2° (166.4°), and the nearest C-H bond exists in the distance of 3.06 Å (3.09 Å) from Mo atom. This structural distortion occurred to relieve the instability of coordinatively-unsaturated Mo centre (16-electron complex) by forming an agostic interaction. This structural distortion was directly observed by single crystal X-ray diffraction measurement for various metals including Cr, Mn, Re and W.[27,47-49] In the case of Mo-PMe_3, on the other hand, structural distortion is not observed and P-Mo-P angle is 175°. The nearest C-H bond is too far (3.90 Å) to interact with Mo vacant site, so there is no agostic interaction to stabilize.

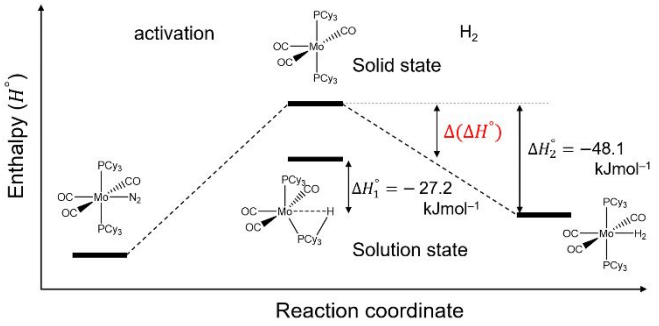

Fig. 5 Energy diagram of H_2 adsorption for the solution state and the solid states (**2**). The value of $\Delta H°_1$ was quoted from ref.28.

Thermodynamic parameters obtained by the DFT calculation are listed in Table S2. From these data, the strength of H_2 adsorption is in the following order; PMe_3 > PCy_3 ≈ $PiPr_3$. This result seems counterintuitive because the order of electron donating ability of phosphine ligand is opposite; PCy_3 ≈ $PiPr_3$ > PMe_3 (Tolman electronic parameter).[50] Usually stronger electron donating ability of the phosphine ligand leads to stronger back donation and stronger binding of dihydrogen ligand. On the basis of experimental and calculation results, energy diagram of H_2 adsorption can be schematized as shown in Fig. 5. In the solution state, molecular motion is relatively free and agostic interaction occurs to stabilize the 16-electron complex, which lowers the energy gap between 16-electron complex and metal-dihydrogen complex ($\Delta H°_1$ in Fig. 5). In the case of **2**, on the other hand, the coordinatively-unsaturated site, which is formed by the N_2 removal, should be fully exposed due to the restricted motion of PCy_3 ligand in the solid state. Therefore, there is no stabilization of the 16-electron complex, which leads to significantly large energy gap between 16-electron complex and metal-dihydrogen complex ($\Delta H°_2$ in Fig. 5).

Here we discuss the difference in the H_2 adsorption isotherms of **2** and previously reported [Mn(CO)(dppe)$_2$][BAr^F_4].[42] Although $\Delta H°$ value is similar (–49 kJ/mol for **2** and –52 kJ/mol for [Mn(CO)(dppe)$_2$][BAr^F_4]), there is a large difference in the adsorbed amount of H_2. The utilization fraction for H_2 adsorption in [Mn(CO)(dppe)$_2$][BAr^F_4] (0.35) is much higher than that of **2** (0.04). This value is too much to be the surface adsorption. Recently, Weller and co-workers reported reversible encapsulation of CH_2Cl_2 and Xe into non-porous organometallic framework [Rh($Cy_2PCH_2PCy_2$)(NBD)][BAr^F_4] (NBD = norbornadiene).[51] They showed that non-covalent interaction of CF_3 group and hydrophobic pathway made by [BAr^F_4]$^-$ anion play an important role of their dynamic porosity. In the case of [Mn(CO)(dppe)$_2$][BAr^F_4], [BAr^F_4]$^-$ anion should also contribute to their dynamic porosity.

Conclusions

In conclusion, we presented H_2 adsorption properties of $[Mo(PCy_3)_2(CO)_3]$ in the solid state synthesized by the two procedures. The sample synthesized *via* the removal of N_2-adduct showed Langmuir type reversible ad/desorption of H_2 above room temperature. Although the adsorption density of H_2 is quite low (0.01 wt%), the N_2 elimination of N_2-adducts is widely applicable. Thus, the current method will be a facile method for evaluating thermodynamic parameters in a series of dihydrogen complexes.

Author Contributions

K. Uchida: investigation, writing-original draft. N. Kishimoto: computation. S. Noro: Gas adsorption. H. Iguchi: conceptualization, writing-review & editing. S. Takaishi: conceptualization, funding, supervision, writing-review & editing, Project administration.

Conflicts of interest

There are no conflicts to declare.

Acknowledgements

This work was partially supported by a JSPS KAKENHI Grant (B) 19H02729, institute for quantum chemical exploration (IQCE), Adaptable and Seamless Technology Transfer Program through Target-Driven R and D (A-STEP, JST) and Tohoku university molecule & material synthesis platform in nanotechnology platform project sponsored by the ministry of education, culture, sports, science and technology (MEXT), Japan.

Notes and references

1 J. Camp, V. Stavila, M. D. Allendorf, D. Prendergast, M. Haranczyk, *J. Phys. Chem. C,* 2018, **122**, 18957.
2 S. Rostami, A. N. Pour, A. Salimi, A. Abolghasempour, *Int. J. Hydrogen Energy,* 2018, **43**, 7072.
3 R. K. Ahluwalia, T. Q. Hua, J. K. Peng, *Int. J. Hydrogen Energy,* 2012, **37**, 2891−2910.
4 K. M. Thomas, *Dalton Trans*., **2009**, 1487−1505.
5 D. E. Jaramillo, H. Z. H. Jiang, H. A. Evans, R. Chakraborty, H. Furukawa, C. M. Brown, M. Head-Gordon and J. R. Long, *J. Am. Chem. Soc.*, 2021, 143, 6248.
6 Y. Liu, H. Kabbour, C. M. Brown, D. A. Neumann and C. C. Ahn, Langmuir, 2008, 24, 4772.
7 M. D. Allendorf, Z. Hulvey, T. Gennett, A. Ahmed, T. Autrey, J. Camp, E. S. Cho, H. Furukawa, M. Haranczyk, M. Head-Gordon, S. Jeong, A. Karkamkar, D. Liu, J. R. Long, K. R. Meihaus, I. H. Nayyar, R. Nazarov, D. J. Siegel, V. Stavila, J. J. Urban, S. P. Veccham, B. C. Wood, *Energy Environ. Sci*., 2018, **11**, 2784.
8 M. Dinca and J. R. Long, *Angew. Chem. Int. Ed*., 2008, 47, 6766-6779.
9 D. Denysenko, M. Grzywa, J. Jelic, K. Reuter, D. Volkmer, *Angew. Chem. Int. Ed*., 2014, 53, 5832.
10 N. Li, Z. Chang, H. Huang, R. Feng, W.-W. He, M. Zhong, D. G. Madden, M. J. Zaworotko, X.-H. Bu, Small, 2019, 15, 1900426.
11 D.-S. Zhang, Z. Chang, Y.-F. Li, Z.-Y. Jiang, Z.-H. Xuan, Y.-H. Zhang, J.-R. Li, Q. Chen, T.-L. Hu, X.-H. Bu, Sci. Rep. 2013, 3, 3312.
12 S. B. Kalidindi, R. A. Fischer, *Phys. Status Solidi B,* 2013, **250**, 1119.
13 A. T. Wijayanta, T. Oda, C. W. Purnomo, T. Kashiwagi, M. Aziz, *Int. J. Hydrogen Energy,* 2019, **44**, 15026−15044.
14 M. V. Lototskyy, M. W. Davids, I. Tolj, Y. V. Klochko, B. S. Sekhar, S. Chidziva, F. Smith, D. Swanepoel, B. G. Pollet, *Int. J. Hydrogen Energy* 2015, **40**, 11491.
15 R. B. Biniwale, S. Rayalu, S. Devotta, M. Ichikawa, *Int. J. Hydrogen Energy* 2008, **33**, 360.
16 T. R. Somo, T. C. Maponya, M. W. Davids, M. J. Hato, M. V. Lototskyy, K. D. Modibane, *Metals,* 2020, **10**, 562.
17 G. J. Kubas, R. R. Ryan, B. I. Swanson, P. J. Vergamini, H. J. Wasserman, *J. Am. Chem. Soc*., 1984, **106**, 451.
18 G. J. Kubas, *Chem. Rev*., 2007, **107**, 4152-4205.
19 G. J. Kubas, *J. Organometallic Chem.*, 2009, 694, 2648-2653.
20 D. M. Heinekey, W. J. Oldham, *Chem. Rev*., 1993, **93**, 913.
21 R. H. Crabtree, *Acc. Chem. Res*., 1990, **23**, 101.
22 R. H. Morris, *Coord. Chem. Rev*., 2008, **252**, 2381-2394.
23 M. Grellier, L. Vendier and S. Sabo-Etienne, *Angew. Chem. Int. Ed*., 2007, **46**, 2613-2615.
24 P. G. Jessop and R. H. Morris, *Coord. Chem. Rev*., 1992, **121**, 155-284.
25 R. H. Crabtree, *Chem. Rev*., 2016, **116**, 8750-8769.
26 S. J. C. Robinson and D. M. Heinekey, *Chem. Commun*., 2017, **53**, 669-676.
27 F. Maseras, A. Lledo´s, E.; Clot, O. Eisenstein, *Chem. Rev*., 2000, **100**, 601.
28 A. A. Gonzalez, K. Zhang, S. P. Nolan, R. L. de la Vega, S. L. Mukerjee, C. D. Hoff, G. J. Kubas, *Organometallics* 1988, **7**, 2429.
29 A. A. Gonzalez, C. D. Hoff, *Inorg. Chem*., 1989, **28**, 4295.
30 R. C. Cammarota, J. Xie, S. A. Burgess, M. V. Vollmer, K. D. Vogiatzis, J. Ye, J. C. Linehan, A. M. Appel, C. Hoffmann, X. Wang, V. G. Young, C. C. Lu, *Chem. Sci*., 2019, **10**, 7029.
31 D. L. M. Suess, C. Tsay, J. C. Peters, *J. Am. Chem. Soc*., 2012, **134**, 14158.
32 D. E. Prokopchuk, G. M. Chambers, E. D. Walter, M. T. Mock, R. M. Bullock, *J. Am. Chem. Soc*., 2019, **141**, 1871.
33 A. Hamaed, M. Trudeau and D. M. Antonelli, *J. Am. Chem. Soc.*, 2008, 130, 6992-6999.
34 T. K. A. Hoang, M. I. Webb, H. V. Mai, A. Hamaed, C. J. Walsby, M. Trudeau and D. M. Antonelli, *J. Am. Chem. Soc.*, 2010, **132**, 11792-11798.
35 A. Hamaed, T. K. A. Hoang, G. Moula, R. Aroca, M. L. Trudeau and D. M. Antonelli, *J. Am. Chem. Soc*., 2011, **133**, 15434-15443.
36 A. I. Cooper and M. Poliakoff, *Chem. Commun*., 2007, 2965.
37 L. Morris, J. Hales, M. Trudeau, P. Georgiev, J. Embs, J. Eckert, N. Kaltsoyannis, D. A. Antonelli, *Energy & Environmental Science,* 2019, **12**, 1580-1591.
38 S. E. Trentowsky, A. J. Lough and R. H. Morris, *Polyhedron*, 2018, 156, 342–349.
39 S. K. Brayshaw, J. C. Green, N. Hazari, J. S. McIndoe, F. Marken, P. R. Raithby and A. S. Weller, *Angew. Chem. Int. Ed*., 2006, 45, 6005-6008.
40 W. Yang, X. Lin, J. Jia, A. J. Blake, C. Wilson, P. Hubberstey, N. R. Champness and M. Schroder, *Chem. Commun*., 2008, 359.
41 G. Alcaraz, M. Grellier and S. Sabo-Etienne, *Acc. Chem. Res*., 2009, **42**, 1640-1649.
42 D. G. Abrecht, B. Fultz, *J. Phys. Chem. C,* 2012, **116**, 22245.
43 R. H. Crabtree, M. Lavin, L. Bonneviot, *J. Am. Chem. Soc*., 1986, **108**, 4032.
44 J. Eckert, G. J. Kubas, R. P. White, *Inorg. Chem*. 1992, **31**, 1550.
45 L. R. Doyle, D. J. Scott, P. J. Hill, D. A. X. Fraser, W. K. Myers,

A. J. P. White, J. C. Green, A. E. Ashley, *Chem. Sci*., 2018, **9**, 7362.
46 M. Brookhart, M. L. Green, L.-L. Wong, *Progr. Inorg. Chem.,* 1988, **36**, 1.
47 K. Zhang, A. A. Gonzalez, S. L. Mukerjee, S. J. Chou, C. D. Hoff, K. A. Kubat-Martin, D. Barnhart, G. J. Kubas, *J. Am. Chem. Soc*., 1991, **113**, 9170.
48 A. Toupadakis, G. J. Kubas, W. A. King, B. L. Scott, J. Huhmann-Vincent, *Organometallics,* 1998, **17**, 5315.
49 D. M. Heinekey, B. M. Schomber, C. E. Radzewich, *J. Am. Chem. Soc*., 1994, **116**, 4515.
50 C. A. Tolman, *Chemical Reviews,* 1977, **77**, 313.
51 A. J. Martínez-Martínez, N. H. Rees, A. S. Weller, *Angew. Chem. Int. Ed*., 2019, **58**, 16873.